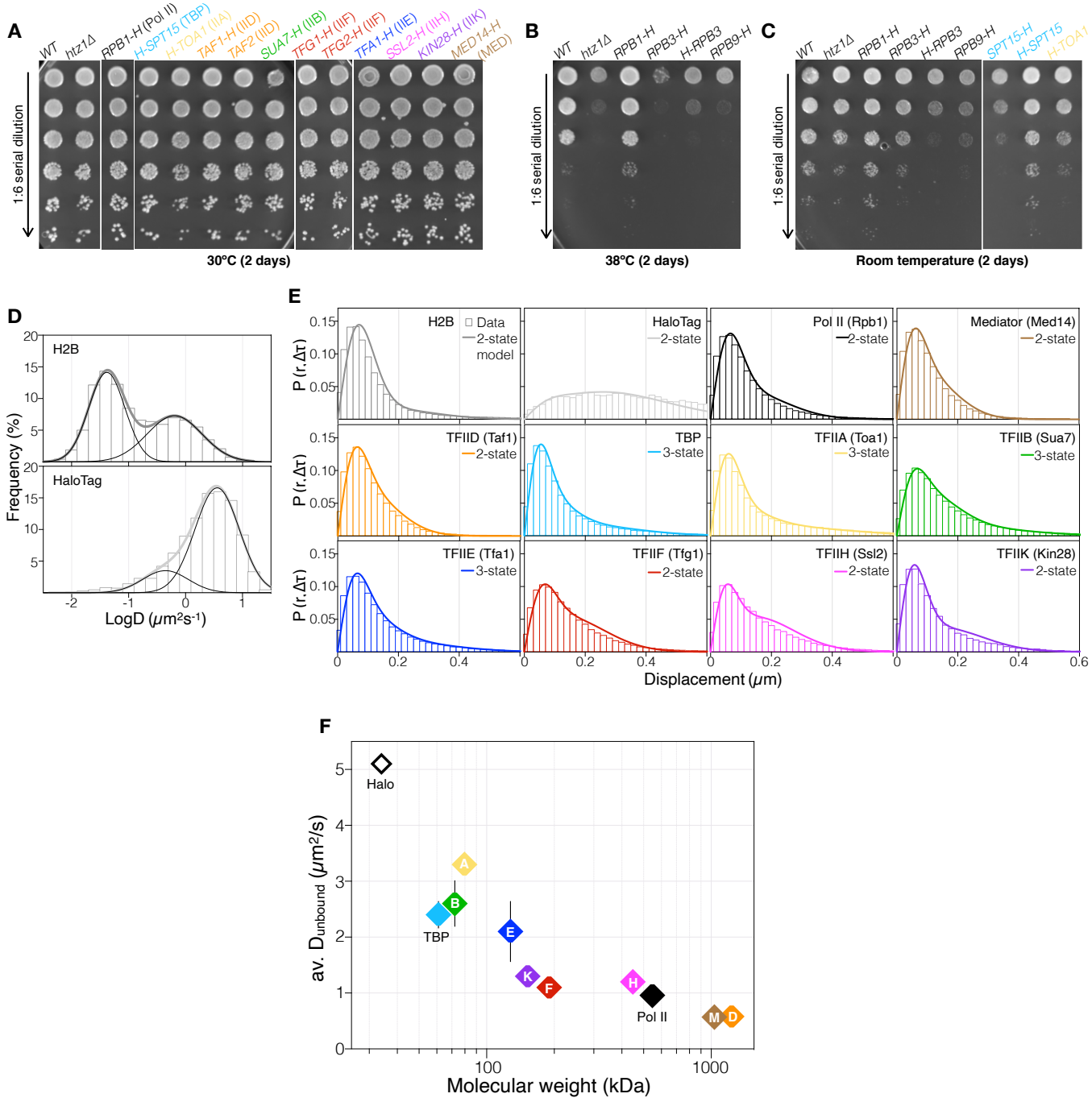

Figure S1. **Global diffusivities of individual PIC components, Related to Figure 1.**
(A) Growth phenotype assay at 30ºC confirming functionality of HaloTag (H) fusions in individual yeast strains. *htz1*Δ strain serves as a control for growth defects under certain conditions. **(B)** and **(C)** C- and N-terminal H fusions of Rpb1 and TBP, respectively, exhibiting wildtype-level growth at 38º (B) or room temperature (C) compared to other genetic permutations. **(D)** LogD histograms (bars), two-Gaussian fits (thick curves) and subpopulations (thin black curves) of H2B (top) and free nuclear HaloTag (bottom). Histograms contain data from three (H2B) or two (HaloTag) biological replicates. **(E)** Displacement (Δt=10 ms) distributions (bars) and corresponding two- or three-state kinetic models (lines). Modeling results are shown in Table S1. Histograms contain data from two (HaloTag) or three (others) biological replicates. **(F)** Correlation between D_{free} (from kinetic modeling) and theoretical molecular weight of each PIC component (log_{10}). D_{free} values, reported in Table S1, are means ± SD from two (HaloTag) or three (others) biological replicates.

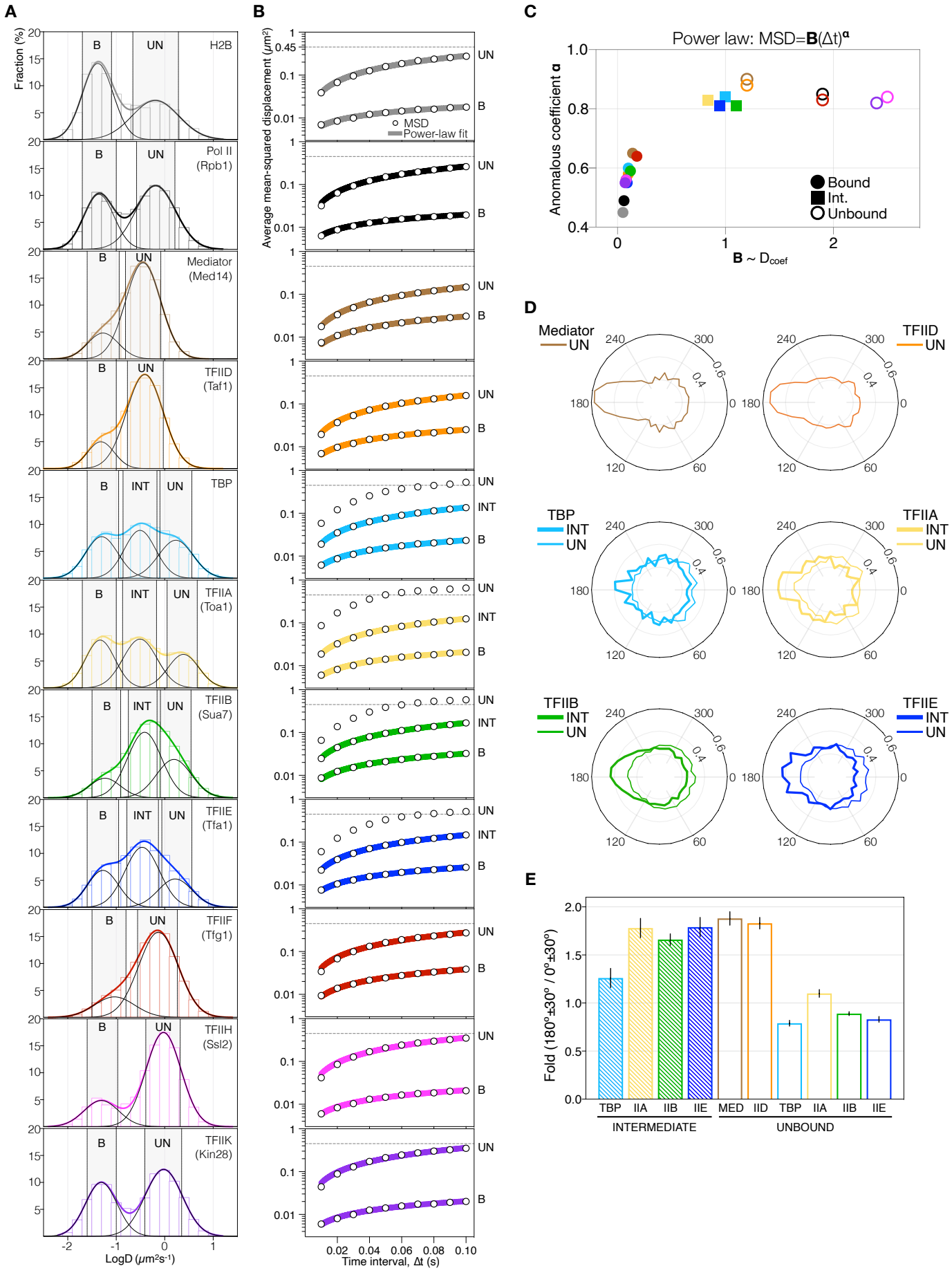
A
B
C
D
E
Fraction (%)
H2B
Pol II (Rpb1)
Mediator (Med14)
TFIID (Taf1)
TBP
TFIIA (Toa1)
TFIIB (Sua7)
TFIIE (Tfa1)
TFIIF (Tfg1)
TFIIH (Ssl2)
TFIIK (Kin28)
B
INT
UN
LogD (μm²s⁻¹)
Average mean-squared displacement (μm²)
MSD
Power-law fit
Time interval, Δt (s)
Power law: MSD=B(Δt)^α
Anomalous coefficient α
B ~ D_coef
Bound
Int.
Unbound
Mediator
TFIID
TBP
TFIIA
TFIIB
TFIIE
Fold (180°±30° / 0°±30°)
TBP
IIA
IIB
IIE
MED
IID
INTERMEDIATE
UNBOUND

Figure S2. **Sub-classification of trajectories and mean-squared displacement (MSD) analysis of distinct dynamic behaviors, Related to Figure 1.**

(A) Fitted logD histograms as in Figure 1C. Trajectories exhibiting D values within mean ± 1 S.D. of respective subpopulation (shaded bars) were selected as a subclass for MSD analysis. B, chromatin-bound. UN, unbound. INT, intermediate. **(B)** Average MSD (log_{10}) computed for each subpopulation and corresponding power-law fit (solid line) of CB and INT. Average MSD plots of free diffusion plateau near the expected MSD ~ 0.45 μm^2 (dashed line, see Methods) for such behavior in the haploid yeast nucleus (0.75 μm radius). **(C)** Power-law fit (equation indicated on top) results showing the anomalous coefficient α, where $\alpha<1$ indicates a subdiffusive behavior, and the constant B, which is proportional to the average $D_{coef.}$ **(D)** Angle analysis for unbound (UN) and intermediate (INT) populations of Mediator, TFIID, TBP, TFIIA, IIB and IIE. Normalized angle distributions were obtained using the vbSPT package (Hansen et al., 2020) (see Methods). **(E)** The probabilities of backward (large 180º±30º angles) relative to forward (small 0º±30º angles) movement, computed based on the angle distributions in (D) (see Methods).

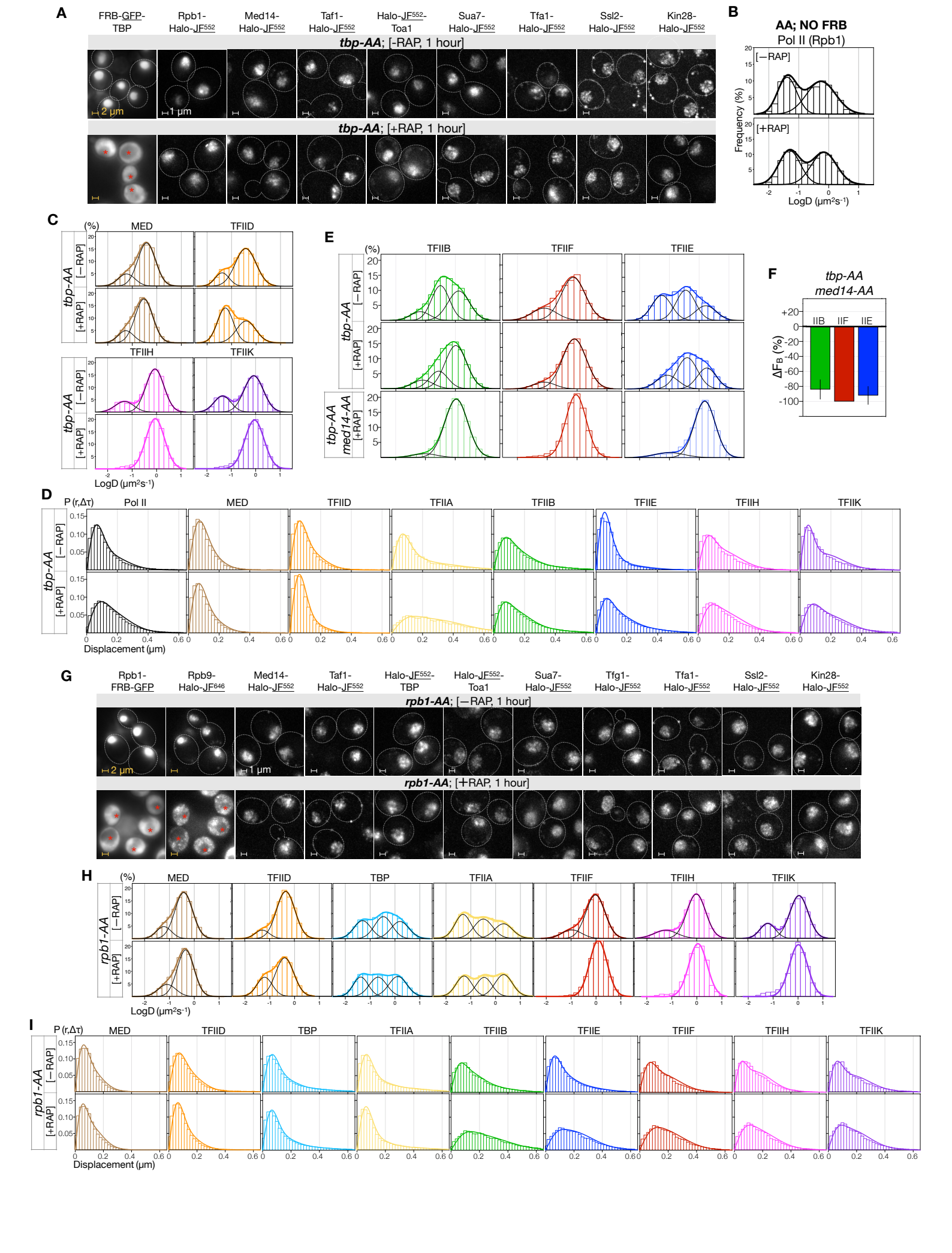
A
FRB-GFP-TBP
Rpb1-Halo-JF552
Med14-Halo-JF552
Taf1-Halo-JF552
Halo-JF552-Toa1
Sua7-Halo-JF552
Tfa1-Halo-JF552
Ssl2-Halo-JF552
Kin28-Halo-JF552
tbp-AA; [-RAP, 1 hour]
tbp-AA; [+RAP, 1 hour]
2 µm
1 µm
B
AA; NO FRB
Pol II (Rpb1)
[−RAP]
[+RAP]
Frequency (%)
LogD (µm²s⁻¹)
C
(%)
MED
TFIID
TFIIH
TFIIK
tbp-AA
[−RAP]
[+RAP]
LogD (µm²s⁻¹)
E
(%)
TFIIB
TFIIF
TFIIE
tbp-AA
tbp-AA med14-AA
[−RAP]
[+RAP]
F
tbp-AA
med14-AA
IIB
IIF
IIE
ΔFB (%)
D
P (r,Δτ)
Pol II
MED
TFIID
TFIIA
TFIIB
TFIIE
TFIIH
TFIIK
tbp-AA
[−RAP]
[+RAP]
Displacement (µm)
G
Rpb1-FRB-GFP
Rpb9-Halo-JF646
Med14-Halo-JF552
Taf1-Halo-JF552
Halo-JF552-TBP
Halo-JF552-Toa1
Sua7-Halo-JF552
Tfg1-Halo-JF552
Tfa1-Halo-JF552
Ssl2-Halo-JF552
Kin28-Halo-JF552
rpb1-AA; [−RAP, 1 hour]
rpb1-AA; [+RAP, 1 hour]
2 µm
1 µm
H
(%)
MED
TFIID
TBP
TFIIA
TFIIF
TFIIH
TFIIK
rpb1-AA
[−RAP]
[+RAP]
LogD (µm²s⁻¹)
I
P (r,Δτ)
MED
TFIID
TBP
TFIIA
TFIIB
TFIIE
TFIIF
TFIIH
TFIIK
rpb1-AA
[−RAP]
[+RAP]
Displacement (µm)

Figure S3. **Effect of TBP and Pol II depletion on dynamics of PIC components, Related to Figure 2.**
(A) Z-projection images showing GFP (TBP) and Halo-JF (others) fluorescence in *tbp-AA* cells before (-RAP, top) and after rapamycin addition (+RAP, bottom). Cell borders are indicated as dashed ovals. Growing cells were treated with DMSO (-RAP) or 1 µg/mL rapamycin (+RAP) for 1 hour before imaging. Imaged fluorescence is underlined. *, vacuole. Scale bar: 2 µm (yellow) and 1 µm (white). **(B)** LogD histograms of Rpb1-Halo in a control Anchor-Away (*AA*) strain harboring no FRB-tagged protein. Rapamycin treatment as described in (A) had little effect on global Pol II dynamics. **(C)** LogD histograms of PIC components in *tbp-AA* cells before (-RAP, top) and after (+RAP, bottom) Pol II depletion, shown as in Figure 2A. Cells were treated as described in (A) before fast tracking for ~2 hours. Histograms contain data from one (-RAP) or two/three (+RAP) biological replicates. **(D)** Kinetic modeling for data in (C) and Figures 2A and 2C, shown as in Figure S1E. Results are reported in Table S2. **(E)** LogD histograms of TFIIB, IIF and IIE before (-RAP) and after (+RAP) TBP depletion (*tbp-AA*), as well as those obtained after simultaneous TBP/Med14 depletion (*tbp-AA*; *med14-AA*). Data are shown as in Figure 2C. **(F)** F_B changes relative to wildtype after double TBP/Med14 depletion, computed and shown as in Figure 2B. **(G)** Z-projection images of PIC components in *rpb1-AA* cells, shown as in (A). **(H)** LogD histograms of PIC components in *rpb1-AA* cells, shown as in (C). **(I)** Kinetic modeling of data in (B) and Figure 2E. Results are reported in Table S2.

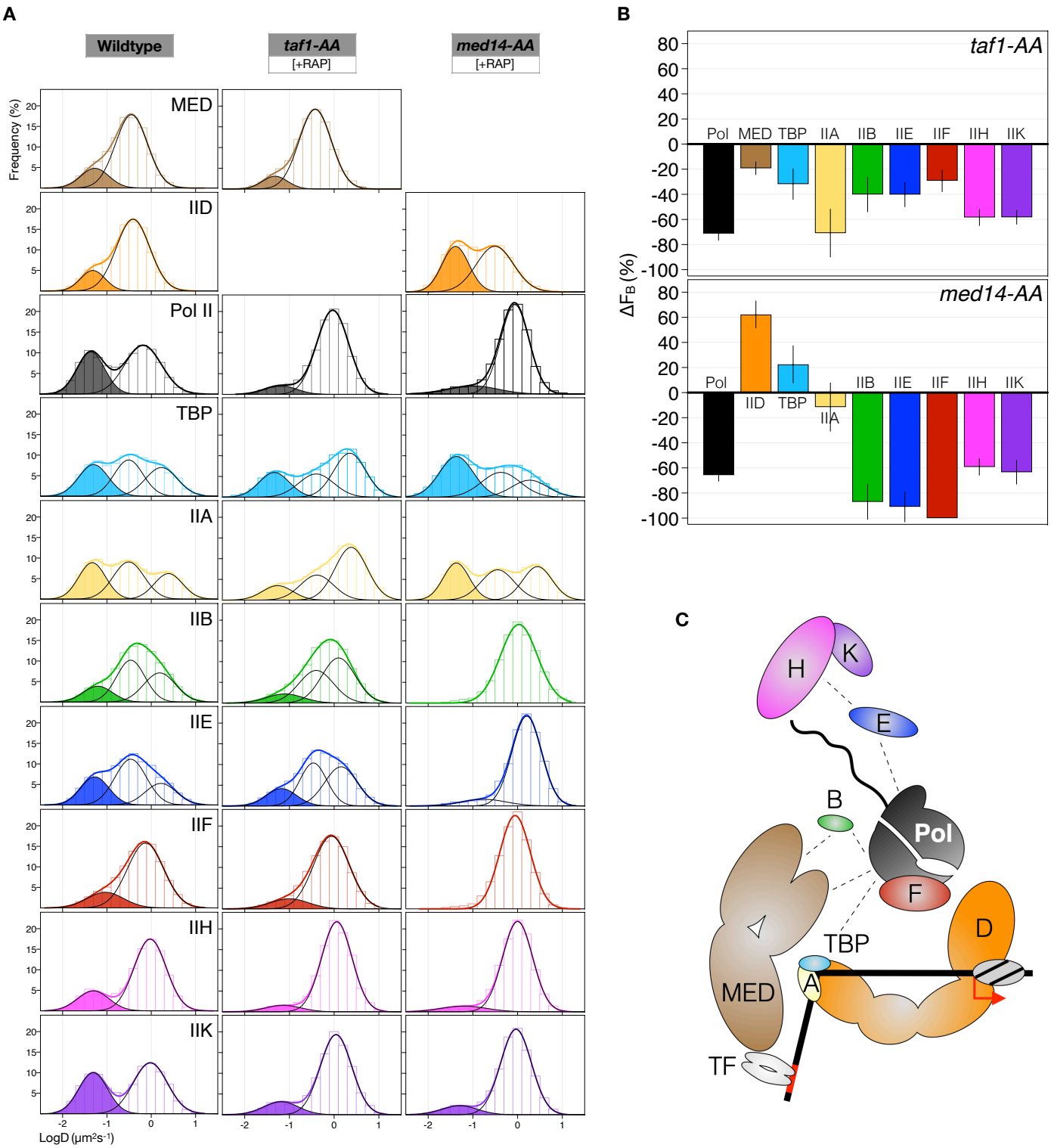

Figure S4. **Effect of Taf1 (TFIID) and Med14 (Mediator) depletion on dynamics of PIC components, Related to Figure 2.** **(A)** LogD histograms of PIC components in wildtype and *taf1-AA* and *med14-AA* cells after 2 and 1 hour of rapamycin treatment, respectively. The chromatin-bound population, resolved through qualitative two- or three-Gaussian fitting, for each component is shaded. Histograms contain data from three (wildtype) or two (*AA*) biological replicates. **(B)** Changes in F_B, determined by kinetic fitting, relative to wildtype after double Taf1 (top) or Med14 (bottom) depletion, computed and shown as in Figure 2B. For *AA* samples, +DMSO control was obtained for one biological replicate each. Fitting results are reported in Table S2. **(C)** A model for hierarchical recruitment of PIC components to chromatin *in vivo*. Mediator, which may be recruited by a bound sequence-specific transcription factor (TF), and Pol II coordinate recruitment of TFIIB, IIE, IIF, IIH and IIK, comprising the enzymatic portion of the PIC. TFIID, TBP and TFIIA recognize and engage promoter elements and assist in recruitment of the enzymatic components. Pol II and TFIIF, as well as TFIIH and IIK, are depicted as subcomplexes prior to recruitment based on previous studies and similar diffusive behaviors observed in live cells (Figures 1F and S2C).

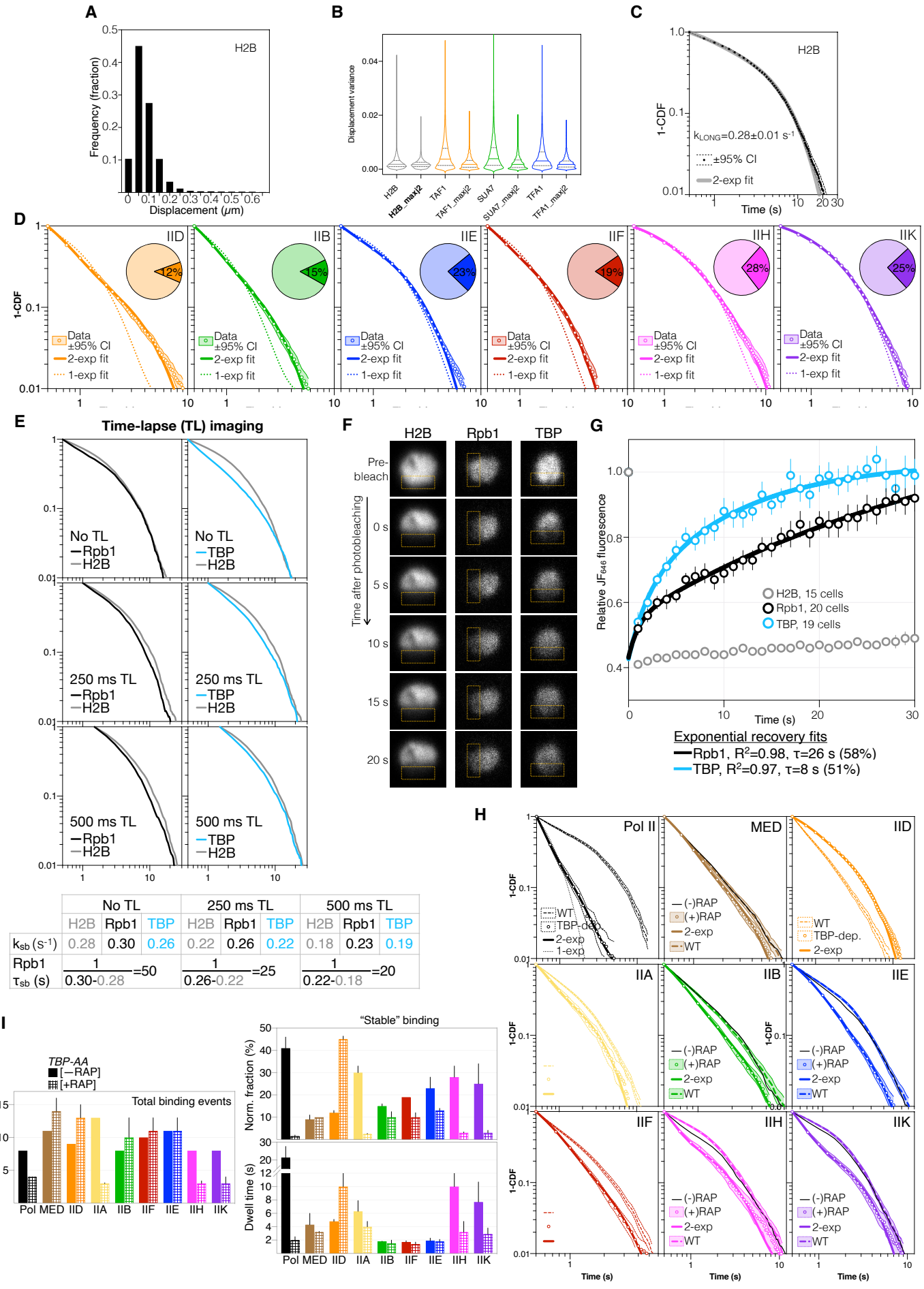

	No TL			250 ms TL			500 ms TL		
	H2B	Rpb1	TBP	H2B	Rpb1	TBP	H2B	Rpb1	TBP
k_{sb} (s^{-1})	0.28	0.30	0.26	0.22	0.26	0.22	0.18	0.23	0.19
Rpb1 τ_{sb} (s)	$\frac{1}{0.30-0.28}=50$			$\frac{1}{0.26-0.22}=25$			$\frac{1}{0.22-0.18}=20$		

Figure S5. **Analyzing slow-tracking and FRAP data, Related to Figure 3.**
(A) Displacement distribution of H2B molecules (Δt=250 ms) showing the motion of chromatin detected by slow tracking. The histogram indicates the predominance of short displacements rarely exceeding 0.2-0.3 μm (~2-3 pixels, 1 pixel = 107 nm). **(B)** Violin plots of variance among displacements by single molecules tracked using a two or three-pixel maximum jump cutoff (see Methods). Trajectories obtained using the two-pixel cutoff exhibit displacement variances similar to that of H2B. **(C)** Log-log 1-CDF curve for H2B, as in (a). The apparent dissociation constant for stable binding k_{sb} from double-exponential fit, used to correct k_{sb} values for PIC components, is indicated. Curve contains data from three biological replicates. **(D)** Log-log survival probability (1-CDF) (dots) computed from apparent dwell times of single-molecule binding events. Re-sampling by bootstrapping provided ±95% confidence interval (CI) (dashed lines). Double-exponential fit (solid line) indicated fractions of stable (f_{sb}) and transient binding (pie chart, f_{sb} shown) and respective apparent unbinding rates (k_{sb} and k_{tb}, Table 1). Curves contain data from three biological replicates. Fit results are reported in Table S1. **(E)** 1-CDF curves for H2B, Rpb1, and TBP acquired by time-lapse imaging (TL) featuring 250 ms exposure time alternating with 250 ms or 500 ms dark time. Results from double-exponential fitting are shown in bottom table. Similar corrected Rpb1 τ_{sb} were obtained from both TL regimes. However, TBP k_{sb} remained too close that that of H2B for correction. **(F)** Raw FRAP images of Halo-H2B, Rpb1-Halo, and Halo-TBP labeled with JF^{646}, showing nuclear fluorescence before (pre-bleach) and up to 20 s after bleaching. The bleach areas are indicated (rectangles). **(G)** Quantitation of fluorescence recovery and corresponding fits for Rpb1 and TBP. Fit quality (R^2) and slow-recovery τ and fraction are indicated for each factor. Data are mean ± s.e.m. from 15 (H2B), 19 (TBP) and 20 cells (Rpb1). The faster TBP recovery is unexpected in light of time-lapse SMT results in (E) and may reflect widely different TBP turnover rates *in vivo*. TBP is highly enriched at Pol I-transcribed genes, where its slow turnover kinetics (Grimaldi et al., 2014; Werven et al., 2009) might be preferentially captured by time-lapse SMT. Further FRAP experiments where the nucleolus, the center of Pol I transcription, is targeted for bleaching may address the discrepancy in these results. **(H)** Slow-tracking results for *tbp-AA* (-) and (+) RAP conditions. Comparing *tbp-AA* (-)RAP and WT curves indicates similar dissociation kinetics. Double-exponential fits are shown for (+) RAP curves and results reported in Table S2. Curves contain data from one (-RAP) or two/three (+RAP and WT) biological replicates and are shown with ±95% CI as in (D). **(I)** Left: Total number of detected binding events (stable and transient) per imaged nucleus under (-) or (+)RAP condition (see Methods). Right: fraction of longer-dwell binding events, normalized for events/nucleus (see Methods) and corrected dwell times.

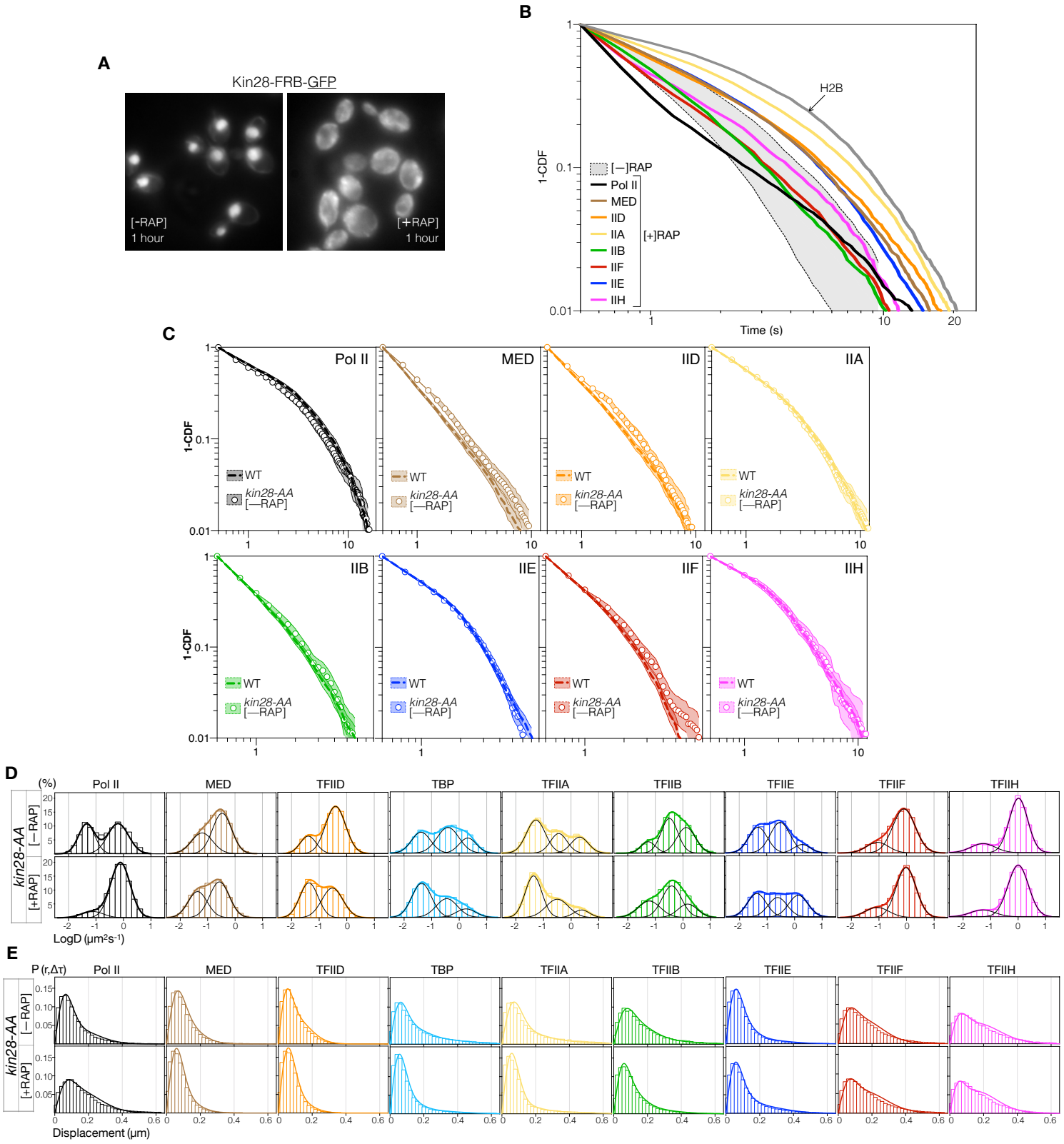

Figure S6. Effect of Kin28 depletion on PIC dynamics, Related to Figure 4.
(A) GFP fluorescence images of Kin28 in *kin28-AA* cells without (-RAP, left) and with (+RAP, right) 1 μg/mL rapamycin for 1 hour. **(B)** Overlay of *kin28-AA* (+RAP) 1-CDF curves from Figure 4C showing extended chromatin residence of Mediator and all GTFs upon Kin28 depletion, compared to the normal range from WT (shaded region). The TFIIA curve approached the H2B limit, precluding reliable photobleaching correction. Thus, we did not quantify and report its dissociation kinetics under this condition. **(C)** Overlay of *kin28-AA* (-RAP) and WT 1-CDF curves for each PIC component showing similar dissociation kinetics. *kin28-AA* and WT data were obtained from one and three biological replicates, respectively. All curves are shown with ±95% CI. **(D)** LogD histograms of PIC components in *kin28-AA* cells, shown as in Figure S3C. **(E)** Kinetic modeling of data in (D). Results are reported in Table S2.

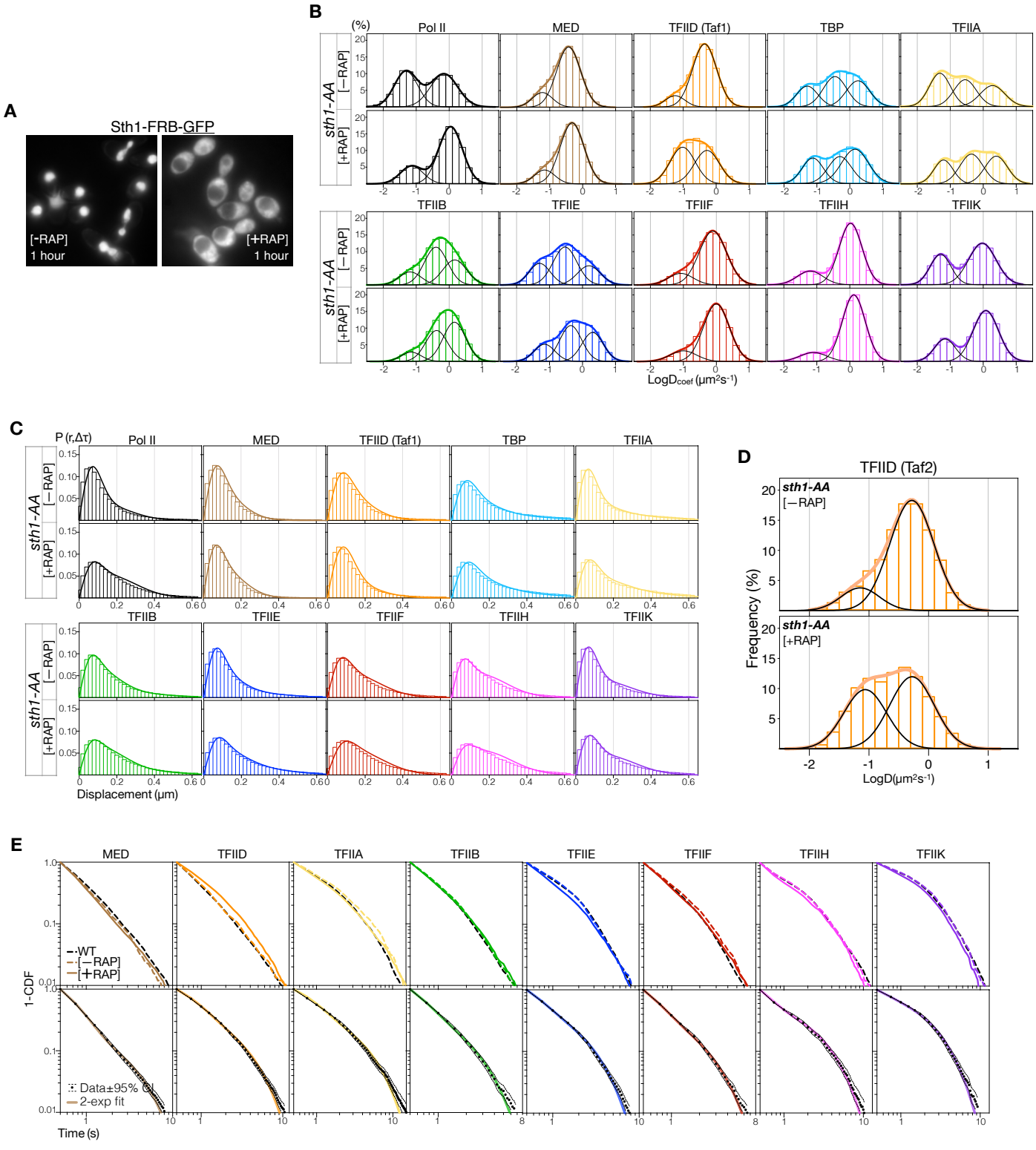

Figure S7. **Effect of RSC inactivation on PIC dynamics, Related to Figure 6.**
(A) GFP fluorescence images of Sth1 in *sth1-AA* cells without (-RAP, left) and with (+RAP, right) 1 μg/mL rapamycin for 1 hour. **(B)** LogD histograms of PIC components in *sth1-AA* cells, shown as in Figure S3C. All histograms contain data from three biological replicates. **(C)** Kinetic modeling of data in (B). Results are reported in Table S2. **(D)** LogD histograms of Taf2 subunit of TFIID showing increased chromatin-bound fraction after RSC inactivation. **(E)** Top: 1-CDF curves for *sth1-AA* (-) and (+) RAP. Comparing *sth1-AA* (-RAP) and WT curves indicates little effect of the *sth1-AA* genetic background on dissociation kinetics of PIC components. Bottom: *sth1-AA* (+RAP) curves, shown with ±95% CI, and corresponding double-exponential fits. Fit results are reported in Table S2. Data were obtained from one (-RAP) and three (+RAP and WT) biological replicates.

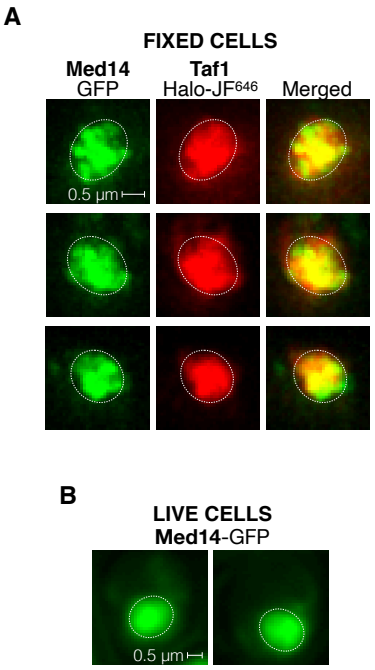

Figure S8. **Nuclear distributions of Mediator and TFIID, Related to Figure 7.**
(A) Two-color deconvolution microscopy images of Med14-GFP (left) and Taf1-Halo-JF^{646} (middle) in three fixed cells showing non-homogenous nuclear distributions. Overlay images (right) show the degree of spatial overlap between prominent Mediator and TFIID foci in the same cells. The approximate nuclear periphery (dashed ovals), based on the overlay image, is indicated for each cell. **(B)** Med14-GFP images obtained from two live cells showing intense signals in subnuclear regions consistent in dimensions with fixed-cell images in (A).

PIC comp.	HaloTag fusion	*WILD-TYPE*																	
		Fast-tracking							Slow-tracking										
		Bound		Intermediate		Unbound		# traj.							N_{trials}	τ_{free} (s)	τ_{search} (s)	SI (s)	Occupancy (%)
		D ($\mu m^2 s^{-1}$)	F_B (%)	D ($\mu m^2 s^{-1}$)	F_I (%)	D ($\mu m^2 s^{-1}$)	F_{UN} (%)		k_{sb} (s^{-1})	τ_{sb} (s)	f_{sb} (%)	k_{tb} (s^{-1})	τ_{tb} (s)	# events					
	Halo-H2B	0.01±0.01	69±3			1.6±0.2	31±3	53,825***	0.28±0.01					6,694***					
	Halo-NLS			0.37±0.03	6±1	5.1±0.1	94±1	14,823**											
Pol II	Rpb1-Halo	0.05±0.00	48±2			1.0±0.1	52±2	50,963***											
Mediator	Med14-Halo	0.06±0.01	39±1			0.6±0.0	61±1	12,725***	0.55±0.11	3.7±1.5	9±3	3.2±0.5	0.3±0.1	5,811***	26±10	0.7±0.5	28.1±9.5	95±40	4±2
TFIID	Taf1-Halo	0.05±0.01	39±3			0.6±0.1	61±3	21,172***	0.49±0.01	4.8±0.3	12±1	3.0±0.2	0.4±0.0	6,700***	22±2	0.9±0.2	28.2±3.6	123±34	4±1
TBP	Halo-Spt15	0.03±0.00	34±4	0.35±0.05	32±0	2.4±0.2	34±4	23,737***											
TFIIA	Halo-Toa1	0.03±0.01	35±6	0.48±0.09	25±2	3.3±0.1	39±7	43,507***	0.44±0.04	6.3±1.6	30±3	2.2±0.2	0.5±0.1	10,125***	7±2	2.4±0.9	21.7±5.5	65±44	10±7
TFIIB	Sua7-Halo	0.05±0.01	21±2	0.55±0.09	44±1	2.6±0.4	35±3	39,191***	0.85±0.01	1.8±0.0	15±1	3.6±0.1	0.3±0.0	4,499***	7±1	2.0±0.3	18.0±2.7	28±9	7±3
TFIIE	Tfa1-Halo	0.04±0.01	33±3	0.39±0.15	36±6	2.1±0.5	31±3	22,235***	0.79±0.10	2.0±0.4	26±5	5.5±1.3	0.2±0.0	8,030***	8±2	0.8±0.3	8.3±1.9	17±2	11±3
TFIIF	Tfg1-Halo	0.05±0.00	25±2			1.0±0.0	75±2	26,932***	0.87±0.07	1.7±0.2	19±0	4.2±0.5	0.3±0.0	5,218***	6±1	1.4±0.2	11.4±1.5	16±8	10±5
TFIIH	Ssl2-Halo	0.06±0.01	27±2			1.2±0.1	73±2	21,134***	0.38±0.04	10.0±4.1	28±5	1.2±0.1	1.1±0.1	4,162***	5±1	6.9±2.2	47.8±13.1	165±47	6±3
TFIIK	Kin28-Halo	0.04±0.00	44±1			1.3±0.0	56±1	9,917***	0.41±0.05	7.7±3.0	25±9	1.0±0.1	1.4±0.2	5,276***	5±2	3.0±1.5	27.2±6.7	100±33	8±4

Table S1. Fast- and slow-tracking results for PIC components in wildtype yeast. Related to Figures 1, S1E, 3 and 5. Fit results from Spot-On kinetic modeling of displacements obtained by fast tracking. Average diffusion coefficients (D) and corresponding fractions of molecules (F) are indicated for distinct populations. Trajectories with at least 3 detections (# traj.) were accounted for in the kinetic model (Figure S1E). Data represent mean ± SD from two or three biological replicates (number of *). For slow-tracking data, double-exponential fitting of the 1-CDF survival curves (Figures 3A, 3B and S4D) was performed to obtain the dissociation rate (k) and corresponding fraction (f) of stably-bound (sb) or transiently-bound (tb) molecules. The dwell times τsb and τtb resulted from correction using ksb for H2B (see Methods). The total number of binding events (transient and stable) from three biological replicates is indicated for each factor. Fast- and slow-tracking data allowed calculations of search kinetics and occupancy according to Figure 5 and STAR Methods.

		Fast-tracking							Slow-tracking					
		Bound		Intermediate		Unbound		# traj.						
		D (μm²s⁻¹)	F_B (%)	D (μm²s⁻¹)	F_I (%)	D (μm²s⁻¹)	F_{UN} (%)		k_{sb} (s^{-1})	τ_{sb} (s)	f_{sb} (%)	k_{tb} (s^{-1})	τ_{tb} (s)	Event #
tbp-AA														
[- RAP]														
Pol II	Rpb1-Halo	0.05	45			0.9	55	14,512*						
Mediator	Med14-Halo	0.04	48			0.47	52	4,387*						
TFIID	Taf1-Halo	0.06	44			0.65	56	5,056*						
TFIIA	Halo-Toa1	0.03	32	0.48	24	3.3	44	10,171*						
TFIIB	Sua7-Halo	0.05	21	0.63	50	2.9	29	6,035*						
TFIIF	Tfg1-Halo	0.05	31			1.2	69	3,744*						
TFIIE	Tfa1-Halo	0.03	45	0.22	30	1.6	25	2,694*						
TFIIH	Ssl2-Halo	0.06	26			1.1	74	5,782*						
TFIIK	Kin28-Halo	0.07	35			1.2	65	7,212*						
[+ RAP]														
Pol II	Rpb1-Halo			0.23±0.06	21±2	1.1±0.1	79±2	46,130***	0.78±0.12	2.0±0.5	3±1	5.1±0.1	0.2±0.0	554*
Mediator	Med14-Halo	0.05±0.00	47±1			0.56±0.02	53±1	22,869***	0.59±0.01	3.2±0.1	8±0	3.1±0.2	0.4±0.0	5,310***
TFIID	Taf1-Halo	0.04±0.01	66±2			0.61±0.14	34±2	22,825***	0.38±0.04	10.0±4.1	31±1	1.9±0.2	0.6±0.1	5,807***
TFIIA	Halo-Toa1			0.36±0.09	13±0	3.6±0.2	87±0	34,469***	0.53±0.05	4.0±0.8	11±0	3.8±0.4	0.3±0.0	925**
TFIIB	Sua7-Halo	0.05±0.00	15±1	0.59±0.07	51±5	2.4±0.2	35±4	37,448***	0.96±0.25	1.5±0.5	8±2	4.0±0.5	0.3±0.0	4,904***
TFIIF	Tfg1-Halo	0.05±0.00	18±2			1.1±0.1	82±2	11,584***	1.02±0.16	1.4±0.3	10±2	3.8±0.8	0.3±0.1	3,682***
TFIIE	Tfa1-Halo	0.04±0.00	19±1	0.40±0.08	39±1	2.0±0.2	42±1	46,172***	0.84±0.10	1.8±0.3	13±1	2.9±0.2	0.4±0.0	4,972***
TFIIH	Ssl2-Halo			0.19±0.03	18±1	1.3±0.1	82±1	28,527***	0.59±0.15	3.2±1.6	8±1	4.9±1.2	0.2±0.1	1,299***
TFIIK	Kin28-Halo			0.20±0.04	20±0	1.4±0.1	80±0	20,657**	0.63±0.11	2.9±0.9	8±3	4.8±0.5	0.2±0.0	1,946***
rpb1-AA														
[- RAP]														
Mediator	Med14-Halo	0.07	39			0.53	61	17,462*						
TFIID	Taf1-Halo	0.07	34			0.69	66	10,718*						
TBP	Halo-Spt15	0.02	32	0.5	35	2.9	33	20,147*						
TFIIA	Halo-Toa1	0.03	37	0.61	27	3.4	36	17,843*						
TFIIB	Sua7-Halo	0.06	18	0.6	46	2.5	36	17,385*						
TFIIF	Tfg1-Halo	0.05	21			1.1	79	18,150*						
TFIIE	Tfa1-Halo	0.05	24	0.46	34	2.1	42	11,735*						
TFIIH	Ssl2-Halo	0.10	22			1.1	78	11,924*						
TFIIK	Kin28-Halo	0.11	26			1.4	74	6,319*						
[+ RAP]														
Mediator	Med14-Halo	0.08±0.00	34±0			0.57±0.02	66±0	34,280***						
TFIID	Taf1-Halo	0.05±0.00	47±1			0.57±0.07	53±1	28,680***						
TBP	Halo-Spt15	0.03±0.00	37±0	0.52±0.05	32±2	2.9±0.3	31±3	34,339**						
TFIIA	Halo-Toa1	0.03±0.00	46±3	0.55±0.01	28±1	3.5±0.1	26±4	35,439***						
TFIIB	Sua7-Halo			0.42±0.08	17±3	2.6±0.3	83±3	44,287***						
TFIIF	Tfg1-Halo			0.24±0.04	10±3	1.5±0.0	90±3	30,982***						
TFIIE	Tfa1-Halo			0.20±0.03	9±3	1.7±0.2	91±3	33,764***						
TFIIH	Ssl2-Halo			0.17±0.04	13±1	1.3±0.1	87±1	29,132***						
TFIIK	Kin28-Halo			0.19±0.03	17±2	1.4±0.0	83±2	23,172***						
kin28-AA														
[- RAP]														
Pol II	Rpb1-Halo	0.05	49			1.0	51	8,680*						
Mediator	Med14-Halo	0.05	48			0.50	52	10,911*						
TFIID	Taf1-Halo	0.06	37			0.53	63	5,320*						
TBP	Halo-Spt15	0.03	32	0.58	35	3.1	33	14,572*						
TFIIA	Halo-Toa1	0.03	40	0.58	27	3.5	33	6,543*						
TFIIB	Sua7-Halo	0.06	25	0.69	51	3.3	24	5,203*						
TFIIF	Tfg1-Halo	0.05	23			1.1	77	6,817*						
TFIIE	Tfa1-Halo	0.03	40	0.29	37	1.8	23	9,662*						
TFIIH	Ssl2-Halo	0.06	18			1.3	82	8,807*						
[+ RAP]														
Pol II	Rpb1-Halo	0.05±0.00	17±1			1.0±0.1	83±1	35,420***	0.38±0.04	10.0±4.1	7±2	4.0±0.7	0.3±0.1	3,028***
Mediator	Med14-Halo	0.03±0.00	67±5			0.43±0.06	33±5	26,376***	0.39±0.04	9.1±3.4	28±2	2.3±0.2	0.5±0.0	8,862***
TFIID	Taf1-Halo	0.03±0.00	66±1			0.43±0.03	34±1	20,698***	0.36±0.01	12.5±2.2	28±2	2.6±0.1	0.4±0.0	6,790***
TBP	Halo-Spt15	0.02	52	0.36	28	2.3	20	20,833*						
TFIIA	Halo-Toa1	0.02±0.00	63±4	0.46±0.06	20±1	3.5±0.3	18±3	32,274***	0.30±0.03	N/A	36±3	1.7±0.2	N/A	8,467***
TFIIB	Sua7-Halo	0.03±0.01	34±1	0.38±0.14	40±4	1.8±0.7	26±4	19,952***	0.53±0.03	4.0±0.5	14±2	2.8±0.1	0.4±0.0	6,202***
TFIIF	Tfg1-Halo	0.05±0.00	20±3			1.1±0.0	80±3	25,221***	0.46±0.01	5.6±0.4	14±1	3.2±0.2	0.3±0.0	3,482***
TFIIE	Tfa1-Halo	0.02±0.00	39±1	0.30±0.07	26±2	1.8±0.1	35±1	35,985***	0.39±0.04	9.1±3.4	31±3	2.4±0.2	0.5±0.0	6,734***
TFIIH	Ssl2-Halo	0.06±0.00	18±2			1.1±0.0	82±2	28,668***	0.45±0.05	5.9±1.8	17±3	3.3±0.7	0.3±0.1	3,288***
sth1-AA														
[- RAP]														
Pol II	Rpb1-Halo	0.04±0.00	51±1			1.1±0.0	49±1	39,142***						

Mediator	Med14-Halo	0.06±0.01	42±2			0.64±0.05	58±2	30,048***							
TFIID	Taf1-Halo	0.06±0.00	36±2			0.72±0.03	64±2	37,412***							
TBP	Halo-Spt15	0.03±0.01	32±3	0.48±0.06	33±1	3.0±0.2	35±2	52,492***							
TFIIA	Halo-Toa1	0.03±0.00	39±1	0.53±0.01	26±0	3.3±0.0	35±0	29,865***							
TFIIB	Sua7-Halo	0.05±0.01	23±3	0.60±0.09	47±4	2.7±0.4	30±5	42,644***							
TFIIF	Tfg1-Halo	0.05±0.00	27±1			1.1±0.1	73±1	35,430***							
TFIIE	Tfa1-Halo	0.03±0.01	32±3	0.36±0.03	34±2	2.0±0.0	34±4	32,023***							
TFIIH	Ssl2-Halo	0.07±0.01	24±2			1.3±0.1	76±2	35,257***							
TFIIK	Kin28-Halo	0.04±0.00	44±5			1.3±0.1	56±5	25,743***							
[+ RAP]															
Pol II	Rpb1-Halo	0.09±0.00	24±2			1.4±0.0	76±2	42,913***							
Mediator	Med14-Halo	0.07±0.01	35±1			0.71±0.02	65±1	27,978***	0.57±0.09	3.4±1.1	9±1	3.3±0.2	0.3±0.0	4,949***	
TFIID	Taf1-Halo	0.04±0.01	54±3			0.80±0.00	46±3	34,683***	0.58±0.09	3.3±1.0	20±2	2.5±0.3	0.5±0.1	6,257***	
TBP	Halo-Spt15	0.03±0.01	26±6	0.56±0.05	28±1	3.1±0.1	46±7	55,291***							
TFIIA	Halo-Toa1	0.04±0.00	24±1	0.65±0.04	28±1	3.2±0.1	48±2	36,911***	0.43±0.04	6.7±1.8	24±2	2.5±0.3	0.5±0.1	4,074***	
TFIIB	Sua7-Halo	0.06±0.02	15±2	0.69±0.01	46±3	2.5±0.0	39±5	39,866***	0.87±0.20	1.7±0.6	16±1	3.8±1.1	0.3±0.1	2,803***	
TFIIF	Tfg1-Halo	0.05±0.00	21±1			1.2±0.1	79±1	49,110***	0.88±0.14	1.7±0.4	21±9	3.6±0.2	0.3±0.0	4,192***	
TFIIE	Tfa1-Halo	0.03±0.02	18±3	0.36±0.03	29±1	2.0±0.0	53±4	36,245***	0.72±0.04	2.3±0.2	20±4	3.5±0.5	0.3±0.0	5,031***	
TFIIH	Ssl2-Halo	0.10±0.01	16±2			1.5±0.1	84±2	38,065***	0.55±0.04	3.7±0.6	32±3	3.0±0.6	0.4±0.1	1,612***	
TFIIK	Kin28-Halo	0.07±0.00	31±3			1.5±0.1	69±3	22,987***	0.67±0.01	2.6±0.1	39±0	4.7±0.1	0.2±0.0	2,660***	

Table S2. Fast- and slow-tracking results for PIC components in AA strains. Related to Figures 2, 4 and 6. Fast- and slow-tracking, when applicable, results from AA experiments, outlined as in Table S1. For tbp-AA, rpb1-AA and kin28-AA, fast-tracking data were collected for one biological replicate under [-RAP] conditions to verify similar dynamics compared to wildtype. For tbp-AA, kin28-AA and sth1-AA, slow-tracking data were collected for one biological replicate under [-RAP] conditions and corresponding 1-CDF curves shown in Figures S4H, S5C and S6E, respectively. Curves were not fitted.

PIC comp.	Subunit	ID	GENOTYPE
WILDTYPE			
		NBY061	***MATa leu2-3,112 trp1-1 can1-100 ura3-1 ade2-1 his3-11,15 [phi+] Δpdr5::LEU2***
Pol II	Rpb1	NBY259	*RPB1-HALO::kanMX6*
Mediator	Med14	NBY229	*MED14-HALO::NatMX*
TFIID	Taf1	NBY150	*TAF1-HALO::NatMX*
TBP	Spt15	NBY212	*HALO-SPT15*
TFIIA	Toa1	NBY280	*HALO-TOA1*
TFIIB	Sua7	NBY079	*SUA7-HALO::NatMX*
TFIIF	Tfg1	NBY154	*TFG1-HALO::NatMX*
TFIIE	Tfa1	NBY152	*TFA1-HALO::NatMX*
TFIIH	Ssl2	NBY081	*SSL2-HALO::NatMX*
TFIIK	Kin28	NBY156	*KIN28-HALO::NatMX*
tbp-AA			
TBP Anchor-Away		**MBY902**	***MATa tor1-1 fpr1::loxP-LEU2-loxP RPL13A-2xFKBP12::loxP pdr5::loxP FRB-GFP-SPT15***
Pol II	Rpb1	NBY332	*RPB1-HALO::NatMX*
Mediator	Med14	NBY339	*MED14-HALO::NatMX*
TFIID	Taf1	NBY334	*TAF1-HALO::NatMX*
TFIIA	Toa1	NBY346	*HALO-TOA1*
TFIIB	Sua7	NBY342	*SUA7-HALO::NatMX*
TFIIF	Tfg1	NBY433	*TFG1-HALO::NatMX*
TFIIE	Tfa1	NBY344	*TFA1-HALO::NatMX*
TFIIH	Ssl2	LBY028	*SSL2-HALO::NatMX*
TFIIK	Kin28	LBY025	*KIN28-HALO::NatMX*
med14-AA			
Med14 Anchor-Away		**NBY439**	***MATa tor1-1 fpr1::loxP-LEU2-loxP RPL13A-2xFKBP12::loxP pdr5::loxP MED14-FRBGFP-KanMX***
Pol II	Rpb1	NBY445	*RPB1-HALO::NatMX*
TFIID	Taf1	NBY459	*TAF1-HALO::NatMX*
TBP	Spt15	NBY483	*HALO-SPT15*
TFIIA	Toa1	NBY489	*MATa tor1-1 fpr1::loxP-LEU2-loxP RPL13A-2xFKBP12::loxP pdr5::loxP KIN28-NatMX MED14_FRBGFP_KanMX HALO_TOA1*
TFIIB	Sua7	NBY472	*SUA7-HALO::NatMX*
TFIIF	Tfg1	NBY473	*TFG1-HALO::NatMX*
TFIIE	Tfa1	NBY476	*TFA1-HALO::NatMX*
TFIIH	Ssl2	NBY496	*SSL2-HALO::NatMX*
TFIIK	Kin28	NBY497	*KIN28-HALO::NatMX*
taf1-AA			
Taf1 Anchor-Away		**NBY349**	***MATa tor1-1 fpr1::loxP-LEU2-loxP RPL13A-2xFKBP12::loxP pdr5::loxP TAF1-FRBGFP-KanMX***
Pol II	Rpb1	NBY359	*RPB1-HALO::NatMX*
Mediator	Med14	NBY363	*MED14-HALO::NatMX*
TBP	Spt15	NBY353	*HALO-SPT15*
TFIIA	Toa1	NBY487	*MATa tor1-1 fpr1::loxP-LEU2-loxP RPL13A-2xFKBP12::loxP pdr5::loxP KIN28-NatMX TAF1_FRBGFP_KanMX HALO_TOA1*
TFIIB	Sua7	NBY357	*SUA7-HALO::NatMX*
TFIIF	Tfg1	NBY494	*TFG1-HALO::NatMX*
TFIIE	Tfa1	LBY040	*TFA1-HALO::NatMX*
TFIIH	Ssl2	NBY361	*SSL2-HALO::NatMX*
TFIIK	Kin28	LBY038	*KIN28-HALO::NatMX*
rpb1-AA			
Rpb1 Anchor-Away		**YAR270**	***MATa tor1-1 fpr1::loxP-LEU2-loxP RPL13A-2xFKBP12::loxP pdr5::loxP RPB1-FRB-GFP::kanMX6***
Pol II	Rpb9	NBY169	*RPB9-HALO::NatMX*
Mediator	Med14	NBY202	*MED14-HALO::NatMX*
TFIID	Taf1	NBY188	*TAF1-HALO::NatMX*
TBP	Spt15	NBY262	*HALO-SPT15*
TFIIA	Toa1	NBY298	*HALO-TOA1*
TFIIB	Sua7	NBY195	*SUA7-HALO::NatMX*
TFIIF	Tfg1	NBY198	*TFG1-HALO::NatMX*
TFIIE	Tfa1	NBY193	*TFA1-HALO::NatMX*
TFIIH	Ssl2	NBY173	*SSL2-HALO::NatMX*
TFIIK	Kin28	NBY199	*KIN28-HALO::NatMX*
kin28-AA			
Kin28 Anchor-Away		**NBY216**	***MATa tor1-1 fpr1::loxP-LEU2-loxP RPL13A-2xFKBP12::loxP pdr5::loxP KIN28-FRB-GFP::kanMX6***
Pol II	Rpb1	NBY323	*RPB1-HALO::NatMX*
Mediator	Med14	NBY250	*MED14-HALO::NatMX*
TFIID	Taf1	NBY144	*TAF1-HALO::NatMX*
TBP	Spt15	NBY265	*HALO-SPT15*
TFIIA	Toa1	NBY302	*HALO-TOA1*
TFIIB	Sua7	NBY312	*SUA7-HALO::NatMX*
TFIIF	Tfg1	NBY149	*TFG1-HALO::NatMX*
TFIIE	Tfa1	NBY314	*TFA1-HALO::NatMX*
TFIIH	Ssl2	NBY128	*SSL2-HALO::NatMX*
sth1-AA			
Sth1 Anchor-Away		**YAR245**	***MATa tor1-1 fpr1::loxP-LEU2-loxP RPL13A-2xFKBP12::loxP pdr5::loxP STH1-FRB-GFP::kanMX6***
Pol II	Rpb1	NBY325	*RPB1-HALO::NatMX*
Mediator	Med14	NBY209	*MED14-HALO::NatMX*
TFIID	Taf1	NBY116	*TAF1-HALO::NatMX*
	Taf2	NBY205	*TAF2-HALO::NatMX*
TBP	Spt15	NBY268	*HALO-SPT15*
TFIIA	Toa1	NBY308	*HALO-TOA1*
TFIIB	Sua7	NBY320	*SUA7-HALO::NatMX*
TFIIF	Tfg1	NBY208	*TFG1-HALO::NatMX*
TFIIE	Tfa1	NBY118	*TFA1-HALO::NatMX*
TFIIH	Ssl2	NBY114	*SSL2-HALO::NatMX*
TFIIK	Kin28	NBY122	*KIN28-HALO::NatMX*

Table S3, related to Key Resources Table. *S. cerevisiae* strains used in this study.

Complex	Subunit	Oligo ID	Oligo sequence
		C-terminal HaloTag	
Pol II	Rpb1	VQN_p12_UP	ATTCTCCAAAGCAAGACGAACAAAAGCATAATGAAAATGAAAATTCCAGAAGTGGAGGCGGAGGTATG
		VQN_p12_DN	AAACTATATATAATGTAATAACGTCAAATACGTAAGGATGATATACTATATCACTATAGGGCGAATTGGGT
Mediator	Med14	MED14_HALONAT_UP	CCTAATGGAAATCCATAATATCCTCAAAGTGGACTCGAACTCAAGTTCATCTAGTGGAGGCGGAGGTATG
		MED14_HALONAT_DN	GGAGAGGGGTTACAATCTCCTAAGGGATAGTAGCGCCGGTGACATTTTATTCGCTACTATAGGGCGAATTGGGTACC
TFIID	Taf1	TAF1_HALOKAN_UP	CAAATAAATCTTGTCCAATGTATAGCAGTAAAGATAACCCTGCTTCACCAAAGAGTGGAGGCGGAGGTATG
		TAF1_HALOKAN_DN	ACAAAACCTTTACAAAAGTTTTATTCGATCAATACATCGTTATACTGAATTCACTATAGGGCGAATTGGGT
	Taf2	TAF2_HALONAT_UP	CACATCAAGATCGTTTATGGTTAAGATAAGAACAAAGAATGATGCTAAGAATAGTGGAGGCGGAGGTATG
		TAF2_HALONAT_DN	GTTTATGTCTATGTATTTGTATAAAATATGATATTACTCAGACTCAAGCAAACAACTATAGGGCGAATTGGGTACC
TFIIB	Sua7	TFIIB_HALOKAN_UP	GCTTATTGCTAATGGTGTAGTGTCTTTGGATAACTTACCGGGCGTTGAAAAGAAAAGTGGAGGCGGAGGTATG
		TFIIB_HALOKAN_DN	CACGAGTACCCGTGCTTCTTGTTCCTATAATTTACTGTTTTATCACTTCATCACTATAGGGCGAATTGGGT
TFIIF	Tfg1	TFG1_HALOKAN_UP	GTAAAAAAATTGTGTCGAAAGGTTGGCAATGACCACATGGAATTAAAGAAAGAGAGTGGAGGCGGAGGT
		TFG1_HALOKAN_DN	GAAAAGAACGAAAACTAAATAACCTATTAAGTACATAACATTATAAACTAACTCACTATAGGGCGAATTGGGT
TFIIE	Tfa1	TFA1_HALOKAN_UP	GATGATGATGATGATGATGATGATGATGAGATGGACATTGAGTTTGAGGACGTTAGTGGAGGCGGAGGT
		TFA1_HALOKAN_DN	GGTTCTACATTGTAAGAGCTAGTTGGTAAGATTTAAAAAAAACGGACCATATCACTATAGGGCGAATTGGGT
TFIIH	Ssl2	SSL2_HALOKAN_UP	CTGAAGGAACATCATCCATTAATCAGAAAGATGTATTATAAGAATTTGAAGAAGAGTGGAGGCGGAGGTATG
		SSL2_HALOKAN_DN	GGTATTATGACTGAATAGATTCAAAATAGGAAGGTGACAATGAAACCAAGCCTATTCACTATAGGGCGAATTGGGT
TFIIK	Kin28	KIN28_HALOKAN_UP	TCAAAGAATTACCACCACCAAGTGACCCGTCTTCAATAAAAATACGTAACAGTGGAGGCGGAGGTATG
		KIN28_HALOKAN_DN	GGATACATCTAATGTCAATAACACAGATTCTACAAATTTTATAAAATCATATCACTATAGGGCGAATTGGGT
		N-terminal HaloTag	
TBP	Spt15	N_TBP_pFA6a_HALO_UP	TCTTTTCTAGTCCAACATAAACAGGTGTATCAAGAGAAACTTTTTTAATTGAATTCGAGCTCGTTTAAACCTC
		N_TBP_pFA6a_HALO_DN	AACACTATCTTGTTTGCCTCTTTAAACTCCTTTAAACGTTCCTCATCGGCACCTCCGCCTCCACTACCGGAAATCTCtAGCGTCGAC
		Promoter_TBP_UP	GCTAAGTGGTATACTTGTGAAATAC
		Promoter_HALO_TBP_DN	CGCCCAGGACTTCCACATAATGGGGGTCGAATGGAAAGCCAGTACCGATTTCTGCCATAATTAAAAAAGTTTCTCTTGATACACC
TFIIA	Toa1	N_TOA1_pFA6a_HALO_UP_2	CGATAGTATCACACAAATCAAGGCCATACACAAGGGACATCGTTGGATATCGCCACTAGTGGATCTGATATCATCG
		N_TOA1_pFA6a_2xGSlinker_HALO_DN	CATTTACCACAGACTCTACGATAATCTCGTACACTCTGCTGGCCTCTGCATTCGATGATCCGCCACCGCCTGAGCCTCCACCACCGGAAATCTCTAGCGTCGAC
		Promoter_TOA1_UP	CGAGCGGTCTAAATCCTGCTTCTCATC
		Promoter_HALO_TOA1_DN	CCAGGACTTCCACATAATGGGGGTCGAATGGAAAGCCAGTACCGATTTCTGCCATGATATCCAACGATGTCCCTTGTG
		C-terminal FRB-GFP tag for Anchor-Away	
Mediator	Med14	MED14_FRBGFP_KAN_UP	TAATGGAAATCCATAATATCCTCAAAGTGGACTCGAACTCAAGTTCATCTGGTGGTGGTGGTGCTAGC
		MED14_FRBGFP_KAN_DN	GGGGTTACAATCTCCTAAGGGATAGTAGCGCCGGTGACATTTTATTCGCTCGACTCACTATAGGGAGACCGGC
TFIID	Taf1	TAF1_FRBGFPKAN_UP	CAAATAAATCTTGTCCAATGTATAGCAGTAAAGATAACCCTGCTTCACCAAAGGGTGGTGGTGGTGCTAGCATC
		TAF1_FRBGFPKAN_DN	CATTATACAAAACCTTTACAAAAGTTTTATTCGATCAATACATCGTTATACTGAATACTATAGGGAGACCGGCAGATC
TFIIK	Kin28	KIN28_FRB_GFPKAN_UP	GTGATTATTTCAAAGAATTACCACCACCAAGTGACCCGTCTTCAATAAAAATACGTAACGGTGGTGGTGGTGCTAGCATC
		KIN28_FRB_GFPKAN_DN	GTTGAGGATACATCTAATGTCAATAACACAGATTCTACAAATTTTATAAAATCATACTATAGGGAGACCGGCAGATC
RSC	Sth1	STH1_FRB_GFPKAN_UP	GATGCTGACAAGTTAAATGAGTTTACTGATGAATGGTTCAAGGAACACTCTTCGGGTGGTGGTGGTGCTAGCATC
		STH1_AIDNAT_DN	GAGGGGAAAGGGATATAGTCGTAAAAAAAAAAAACATGTGGTGATGAAAACGCTATAGGGAGACCGGCAGATC
		N-terminal FRB-GFP tag for Anchor-Away	
TBP	Spt15	N_TBP_pFA6a_HALO_UP	TCTTTTCTAGTCCAACATAAACAGGTGTATCAAGAGAAACTTTTTTAATTGAATTCGAGCTCGTTTAAACCTC
		N_TBP_pFA6a_FRBGFP_DN	AACACTATCTTGTTTGCCTCTTTAAACTCCTTTAAACGTTCCTCATCGGCACCTCCGCCTCCACTGCCACCGCCTGAACCGCCTCC
		Promoter_TBP_UP	GCTAAGTGGTATACTTGTGAAATAC
		Promoter_FRBGFP_TBP_DN	CAAACGAGATGCCTCTTCCAGGCCTTCATGCCACATCTCATGCCAGAGGATCATAATTAAAAAAGTTTCTCTTGATACACC

Table S4, related to Key Resources Table. Oligonucleotides used in this study for tagging PIC components.